

**MeV electrons detected by the Alice UV
spectrograph during the New Horizons flyby of
Jupiter**

A. J. Steffl¹, A. B. Shinn¹, G. R. Gladstone², J. Wm. Parker¹,
K. D. Retherford², D. C. Slater^{2,†}, M. H. Versteeg², S. A. Stern³

[†] Deceased 30 May 2011

A. J. Steffl, A. B. Shinn, J. Wm. Parker, and S. A. Stern, Southwest Research Institute, 1050
Walnut St., Suite 300, Boulder, CO 80302-5150, USA. (steffl@boulder.swri.edu)

G. R. Gladstone, K. D. Retherford, and M. H. Versteeg, Southwest Research Institute, P. O.
Drawer 28510, San Antonio TX 78228-0510, USA.

¹Department of Space Studies, Southwest
Research Institute, Boulder, Colorado, USA.

²Space Science and Engineering Division,
Southwest Research Institute, San Antonio,
Texas, USA.

³Space Science and Engineering Division,
Southwest Research Institute, Boulder,
Colorado, USA.

Abstract. In early 2007, the *New Horizons* spacecraft flew through the Jovian magnetosphere on the dusk side. Here, we present results from a novel means of detecting energetic electrons along *New Horizons*' trajectory: the background count rate of the Alice ultraviolet spectrograph. Electrons with energies >1 MeV can penetrate the thin aluminum housing of Alice, interact with the microchannel plate detector, and produce a count that is indistinguishable from an FUV photon. We present Alice data, proportional to the MeV electron flux, from an 11-day period centered on the spacecraft's closest approach to Jupiter, and compare it to electron data from the PEPSSI instrument. We find that a solar wind compression event passed over the spacecraft just prior to it entering the Jovian magnetosphere. Subsequently, the magnetopause boundary was detected at a distance of $67 R_J$ suggesting a compressed magnetospheric configuration. Three days later, when the spacecraft was $35\text{--}90 R_J$ downstream of Jupiter, *New Horizons* observed a series of 15 current sheet crossings, all of which occurred significantly northward of model predictions implying solar wind influence over the middle and outer Jovian magnetosphere, even to radial distances as small as $\sim 35 R_J$. In addition, we find the Jovian current sheet, which had a half-thickness of at least $7.4 R_J$ between 1930 and 2100 LT abruptly thinned to a thickness of $\sim 3.4 R_J$ around 2200 LT.

1. Introduction

The *New Horizons* spacecraft, the first of NASA’s New Frontiers program, will be the first to flyby the Pluto system [Stern, 2008]. In early 2007, *New Horizons* flew past Jupiter on a gravity assist trajectory that will bring it to its closest approach with Pluto on 14 July 2015. This flyby provided a unique opportunity to study the Jovian magnetosphere and its response to a large increase in the dynamic pressure of the solar wind. The spacecraft approached Jupiter from the direction of late morning local time. *New Horizons*’ closest approach to Jupiter occurred at 05:43:41 UTC on 28 February 2007 (DOY 059) on the dusk side of Jupiter at a distance of 32.2 R_J . The outbound trajectory was nearly aligned with the anti-solar direction, which enabled NH to fly down the Jovian magnetotail out to distances greater than 2500 R_J [McComas et al., 2007; McNutt et al., 2007]. The trajectory of *New Horizons* around closest approach to Jupiter is shown in Fig. 1.

The Alice FUV spectrograph on *New Horizons* consists of a small telescope (4 cm x 4 cm) with an opaque aperture door that feeds a Rowland circle spectrograph with a microchannel plate (MCP) detector and the associated electronics [Stern et al., 2008]. These components are housed inside an aluminum case just 1.3 mm (50 mils) thick. During the Jupiter flyby, the Alice FUV spectrograph made numerous observations of Jupiter, the Galilean satellites, and the Io plasma torus over an 11-day period from day 053–064. After day 064, the angle between Jupiter and the Sun, as seen from *New Horizons*, dropped below 20°, precluding further FUV observations. Results from Alice FUV observations of the Jovian system have been presented by Gladstone et al. [2007], Retherford et al. [2007], and Greathouse et al. [2010].

Alice is mounted to an exterior panel of the *New Horizons* spacecraft, where it is directly exposed to the local energetic particle environment. Incident particles from nearly 2π steradians (the spacecraft body provides shielding for the other 2π steradians) can strike the instrument and, if they have energies greater than 680 keV for electrons or 15 MeV for protons, penetrate the relatively thin instrument housing. At Jupiter, the flux of electrons with energy greater than 680 keV is several orders of magnitude greater than the flux of protons with energy greater than 15 MeV [*Baker and van Allen, 1976; Schardt et al., 1981*], so the penetrating energetic particles will be dominated by electrons. Since the energetic particle flux at Pluto is expected to be low, no additional attempt was made to shield the detector. As a result, some fraction of the penetrating energetic particles (or the secondary gamma-rays/x-rays they produce) are scattered in such a way that they interact with the MCP detector to produce a count that is indistinguishable from one made by a FUV photon. In this way, Alice can act as a third *in situ* particle detector and complement the two dedicated particles instruments on *New Horizons*, PEPSSI and SWAP. During the Jupiter flyby, Alice demonstrated that it is quite effective at detecting energetic electrons—at times generating more than 15,000 counts s^{-1} .

PEPSSI, the Pluto Energetic Particle Spectrometer Science Investigation, is a multi-directional, time-of-flight spectrometer that measures energetic electrons and ions [*McNutt et al., 2008*]. We use PEPSSI electron data for comparison to the Alice energetic particles data and during times when Alice data are not available. PEPSSI contains three separate electron detectors, each with a field of view of approximately $12.5^\circ \times 12^\circ$, oriented in three separate look directions. Each detector measures electron fluxes in three energy ranges: 25–190 keV, 190–700 keV, and 700–1000 keV. Although PEPSSI can operate with an

integration period as short as 1s, during the Jupiter flyby, the integration period was generally 60s, although there were several short periods where a 15s integration period was used.

1.1. Jovian Coordinate Systems

In this paper we use two different body-centered, non-inertial coordinate systems: cylindrical System III (1965) and Cartesian Jupiter-Sun-Orbital (JSO). System III (1965), usually referred to as just “System III”, is a coordinate system that rotates with (or nearly with) Jupiter. It is defined such that the +Z axis is aligned with Jupiter’s north rotational pole, while the X and Y axes rotate with the planet at a rate of 870.536° per ephemeris day [Riddle and Warwick, 1976]. By tradition, System III is a left-handed system, such that the longitude of an observer fixed in inertial space increases with time.

JSO is a Cartesian coordinate system defined such that the +X axis is the instantaneous vector from Jupiter to the Sun and the Z axis is perpendicular to Jupiter’s orbital plane, with +Z pointing close to Jupiter’s north pole of rotation. The Y axis is perpendicular to the other two axes to complete the triad, with positive Y pointing approximately in the direction opposite of Jupiter’s orbital motion. To minimize confusion, an uppercase “Z” will refer to the System III coordinate system while a lowercase “z” will refer to the JSO coordinate system.

2. Sensitivity of Alice to energetic particles

There are two primary mechanisms through which Alice can detect energetic particles: direct impingement on the MCP and FUV fluorescence induced in the MgF_2 window located just in front of, and at 90° to, the front surface of the MCP (cf. Fig. 5 in Stern

et al. [2008]). To quantify the detection efficiency of these two mechanisms, testing was performed on the flight spare detector of the *Rosetta* Alice spectrograph (the flight spare detector for *New Horizons* Alice was used as the flight detector for the LAMP instrument on the Lunar Reconnaissance Orbiter) at the Goddard Space Flight Center Radiation Effects Facility (REF) in September 2003. The *Rosetta* Alice flight spare detector is very similar to the *New Horizons* Alice flight detector and the input surface of the *Rosetta* Alice MCP was re-coated using the same KBr and CsI photocathodes and layout as used with *New Horizons* Alice. The spare detector was placed in the REF beam line and irradiated with 1 MeV electrons. The detection efficiency was found to be 0.33 for direct irradiation of the MCP with MeV electrons and 0.012 for irradiation of the MgF₂ window. In addition, it was confirmed that the detector is sensitive to gamma-rays produced by the REF. Although not directly measured for this detector, similar MCP detectors have quantum efficiencies of approximately 2% for X-rays/gamma-rays with energies between 50-2000 keV (O. Siegmund, personal communication, 2003).

The count rate of the detector was linear with the flux of particles. In addition, the observed variance of the Alice data matches the theoretical prediction for Poisson-distributed events and a detector with a non-paralyzable dead time [Lucke, 1976]. This strongly implies (but does not strictly prove) that when an energetic electron interacts with the detector, it produces a single count, rather than multiple counts, which would be correlated.

We used the the Multi-LAyered Shielding Simulation Software (MULASSIS) [Lei *et al.*, 2002] as implemented by the Space Environment Information System (SPENVIS) [Heynderickx *et al.*, 2001] to model the flux of penetrating electrons and secondary photons

(X-rays and gamma-rays) through the interior wall of the instrument housing as a function of initial electron energy over the range of 0.05-64 MeV in 20 logarithmically spaced steps. By multiplying the flux of penetrating electrons and secondary photons at each energy level by the electron flux observed in the middle/outer magnetosphere of Jupiter [Baker and van Allen, 1976] and the above detection efficiencies, we obtain an estimate of the energy range of electrons most likely to produce Alice counts at Jupiter, shown in Fig. 2. 91% of the Alice counts result from penetrating electrons with initial energies between 1–8 MeV, with the most probable energy range being 2-2.8 MeV. Electrons with initial energies less than 1 MeV accounted for a scant 0.2% of the total simulated counts. Secondary photons produced by electrons of all initial energies accounted for just 1% of the total Alice counts, but 96% of the counts produced by electrons with initial energies less than 1 MeV.

3. Alice Data and Analysis

During the Jupiter flyby, the Alice FUV spectrograph made observations of Jupiter, the Galilean satellites, and the Io plasma torus over an 11-day period from day 053–064. After day 064, the angle between Jupiter and the Sun, as seen from *New Horizons*, dropped below 20°, precluding further FUV observations. Results from Alice FUV observations of the Jovian system have been presented by Gladstone et al. [2007], Retherford et al. [2007], and Greathouse et al. [2010].

Typically, Alice FUV observations lasted about one hour and were separated by several hours. To avoid repeated cycling of the instrument’s high voltage power supply between planned observations, Alice was often left powered-on at the nominal high voltage level but with its opaque aperture door closed. In this state, Alice was sensitive to photons

(or energetic particles), but external FUV photons could not reach the detector. In total, Alice spent 37.0% of the time between DOY 053.7-064.0 like this.

Whenever Alice is on, it records housekeeping (HK) data at a programmable rate. During the Jupiter flyby, this rate was once per second. In addition to information about the health of the instrument and its current operating state, the HK data contain the total detector count rate. Although lacking any spatial or spectral information, this data allows the instrument to act as a simple photometer, even when it is not taking actively commanded exposures.

As a safety measure, if the count rate recorded in the Alice HK data ever exceeds a programmable value, the instrument will end any currently active exposure, turn off the detector high voltage, and enter “safe” mode for a period of 15 minutes. After the safety timeout expires, the detector high voltage remains off and Alice is incapable of detecting photons or energetic particles until it receives a command to make an exposure or otherwise ramp up the high voltage to operational levels. At the start of the Jupiter flyby period, the Alice count rate safety value was set to 15,000 counts s⁻¹. When *New Horizons* first entered the Jovian magnetosphere, Alice repeatedly exceeded this count rate limit, resulting in a significant loss of data on days 057–059. At 2007-059T18:01:17, roughly 12 hours after closest approach, the Alice count rate limit was raised to 35,000 counts s⁻¹. However, the observed count rate did not exceed the original limit of 15,000 counts s⁻¹ (hereafter cps) for the remainder of the flyby.

3.1. Detector Dead Time

When a charge cloud from the MCP hits the Alice double delay line (DDL) readout anode, the detector electronics take a small, but non-zero, amount of time to process

the event. During this time, the detector cannot process any additional events, i.e., it is “dead”. This dead time introduces a non-linearity to the detector response which becomes more significant at higher count rates. Since the Alice detector operates in the non-paralyzable regime the relationship between the true count rate and the observed count rate is:

$$C_{true} = \frac{C_{obs}}{1 - \tau C_{obs}} \quad (1)$$

where τ is time constant of the electronics. (See *Knoll* [1979] for further discussion of detector dead time and paralyzable versus non-paralyzable dead time). The time constant of the Alice HK electronics was measured in the lab and in-flight to be 4 μ s. Thus, the maximum dead time correction factor during the Jupiter flyby is 1.064, for an observed HK count rate of 15,000 cps.

3.2. Detector Background Count Rate

Whenever the Alice detector is in its nominal operating state, it produces counts at a low rate—even if the aperture door is closed and no FUV photons can reach the detector. Primarily, these background counts are caused by gamma rays from the spacecraft’s RTGs striking the detector, although radioactive decay in the MCP glass and noise in the detector electronics also contribute. The intrinsic background count rate of Alice was measured in August 2006, January 2007, and July 2007 and found to be constant, to within 5%, with an average value of 104 counts s^{−1}. After correcting the Alice count rate data for detector dead time, we subtract this value from the data.

In addition to the intrinsic background count rate, the detector electronics can be commanded to produce artificial events or “stims pulses”, at fixed locations on opposite

ends of the readout anode. These stim pulses aid in determining the location of where charge pulses from the MCP strike the readout anode. When they are on, the stim pulses produce counts at a constant rate of 36 counts s^{-1} , which we subtract from the count rate data.

3.3. FUV photons

When the Alice aperture door is closed, all of the detected counts are due to either the intrinsic background count rate (which only varies on timescales of months or longer) or interactions with energetic particles. The situation becomes more complicated when the aperture door is open and several thousand counts per second are produced by FUV photons. We exclude from our analysis all periods when Alice is observing a target that is known to vary rapidly with time (e.g., the Jovian aurora or the Io plasma torus) or when the spacecraft pointing is not constant during an observation, as in a scan. For the remaining periods when the Alice aperture door is open, we estimate the count rate due to FUV photons by comparing the mean count rate during the 15 seconds immediately prior to opening the aperture door to the mean count rate in the 15 seconds immediately after. We attribute the increase in count rate when the door is opened to be due solely to FUV photons. Likewise, we compare the mean count rate during the 15 seconds immediately before and after the aperture door was closed. We require the FUV photon count rate derived at the beginning of the door open period to be within 25% of the photon count rate at the end of the door open period. If this condition is met, we assume that any variations in the FUV photon count rate with time are small enough that they can be approximated by a linear fit and then subtract off this fitted count rate from the dead time corrected data. As seen in Figs. 3, 5, and 7 below, count rate data obtained with

the aperture door open and corrected in this way closely matches the count rate data obtained with the aperture door closed.

4. Why use an FUV spectrograph to measure MeV electrons?

Alice was clearly not designed to serve as an energetic electron detector. It has no means of determining the spatial distribution of energetic electrons nor does it have any capability to measure their energy, save for the low energy cutoff required to penetrate the instrument housing. Since the efficiency of detecting energetic electrons depends on both of these, there is no way to reliably convert the Alice count rates into units differential flux—although the count rate will be proportional to the integrated flux. Given these rather significant drawbacks and the presence of a dedicated energetic electron instrument onboard *New Horizons*, why is the Alice electron data worth examining?

There are several reasons. Chief among these is that Alice is the only instrument on *New Horizons* sensitive to electrons with energies greater than 1 MeV. (Since electrons with these energies are not expected at Pluto, PEPSSI was not designed to measure them.) Thus, Alice provides electron measurements in a complimentary energy range. Second, there are several periods during the 11-day period around closest approach when Alice was collecting data but PEPSSI was either not powered on or was operating at off-nominal instrument settings. Third, *New Horizons* was operated in 3-axis stabilized mode until DOY 82. With three electron detectors that have a $12.5^\circ \times 12^\circ$ field of view, PEPSSI sampled only a small fraction of the total 4π steradians. Thus, PEPSSI could easily miss (or undercount) a source of energetic electrons that is collimated and not omnidirectional. If there are such collimated electrons, the PEPSSI count rates will be quite sensitive to changes in spacecraft pointing, and indeed, at times there are strong correlations between

PEPSSI count rates and spacecraft attitude. The roughly hemispheric coverage of Alice makes it less likely to miss a collimated source, and less sensitive to small changes in pointing. Fourth, the Alice count rates from MeV electrons are 100–300 times greater than the count rates in the highest energy bin of the PEPSSI electron detectors, resulting in a higher signal-to-noise ratio (due to Poisson noise). Alice data also have 16 bits of linear dynamic range, whereas PEPSSI electron data have 10 bits of logarithmically scaled dynamic range. This results in the number of electron events recorded in each PEPSSI integration period being quantized by the six most significant bits needed to represent a given integer value. For example, the following are sequences of three consecutive event counts that PEPSSI can store: [61, 62, 63], [64, 66, 68], [128, 132, 136], [1024, 1056, 1088], etc. This introduced an uncertainty of up to 3% in the true count rate. Finally, the Alice data are sampled with 1s time resolution, compared to 60s time resolution for most of the PEPSSI electron data at Jupiter.

5. Results

Over a 11-day period, beginning on DOY 053 and roughly centered on the spacecraft’s closest approach to Jupiter, Alice recorded 328,954 measurements of the count rate with the aperture door closed. An additional 61,977 measurements were recorded when the aperture door was open and the correction for FUV photons could be applied. These measurements cover 44% of the total elapsed time during this period. The dead time corrected, background subtracted Alice HK count rate during the Jupiter encounter is shown in Fig. 3. Data points plotted in red represent times when the Alice aperture door was open and the FUV photon count rate has been subtracted as described in Section 3.3, above. Since, in all cases, the FUV count rate subtracted from data obtained

with the aperture door open was several thousand counts s^{-1} , these data have a much larger variance than data obtained nearby in time, but with the aperture door closed.

5.1. Upstream Solar Wind Conditions

Prior to crossing the Jovian magnetopause, the *New Horizons* spacecraft was immersed in the ambient solar wind plasma. Alice remained off during the distant approach to Jupiter until DOY 053. However, PEPSSI did take data during this period, and from DOY 040, at a distance of 442 R_J upstream Jupiter, until DOY 053, 134 R_J upstream Jupiter, the electron detectors on PEPSSI show a gradual 15% increase in the flux of energetic electrons. Given the long duration of this increase and correlation with distance, the only plausible source of these electrons is the Jovian magnetosphere. A similar enhancement of energetic particles was seen by the *Voyager* spacecraft on approach to Jupiter [Baker et al., 1984]. When Alice started taking data on DOY 053 at 16:00, the average count rate was 10 cps higher than the intrinsic background rate of 104 cps, indicating the presence of a detectable flux of Jovian energetic electrons.

Results from the Michigan Solar Wind Model (mSWiM) which uses measurements at Earth to propagate solar wind conditions to Jupiter using a 1-D MHD code [Zieger and Hansen, 2008], predicted that a large solar wind compression event would reach Jupiter on DOY 051 \pm 1. Two days later, on DOY 053, the Solar Wind Around Pluto (SWAP) instrument on New Horizons [McComas et al., 2008], observed a solar wind forward shock followed by an increase in solar wind protons, consistent with the arrival of this event [Elliott et al., 2007]. This solar wind event seems responsible for the sharp increase in the brightness of the Jovian FUV aurora observed by HST on DOY 054 and 055 [Clarke et al., 2009]. After adjusting the propagated arrival times by 2.1 days to match the

SWAP observation of the solar wind forward shock, mSWiM predicts a sharp rise in solar wind density at the position of *New Horizons* beginning at DOY 054.8 with a peak solar wind density occurring at DOY 055.1. PEPSSI was taking data throughout this period, and beginning on DOY 054.9, each of the PEPSSI's three electron detectors measured a significant increase in the flux of energetic electrons. 14 hours of Alice count rate data are also available during the period of peak solar wind density, as shown in Fig. 4. The ratio of electron flux at the peak of the solar wind event to the pre-event background rate is 9.4 for Alice and 4.0, 3.3, and 3.1 for the high, medium, and low energy ranges of the PEPSSI E0 detector, implying that the electron energy spectrum in the solar wind flow was significantly harder than in the ambient plasma consisting of electrons coming from Jupiter.

The Alice count rate during this period is highly correlated with the observed energetic electron fluxes from all three of the PEPSSI electron detectors. The correlation is strongest for the PEPSSI E0 detector. Geometrically, this makes sense, since the E0 detector has its field of view in the same hemisphere of the sky as Alice (the +Z hemisphere, in spacecraft coordinates). The PEPSSI E1 and E2 detectors both have their boresight vectors at an angle of -22° relative to the spacecraft X-Y plane, and electrons from this hemisphere would have to pass through the spacecraft body before reaching Alice. The Pearson linear correlation coefficient between Alice and the PEPSSI E0 data is 0.88 for 25-190 keV electrons, 0.95 for 190-700 keV electrons, and 0.86 for 700-1000 keV electrons bin. In this case, the low correlation coefficient for the highest PEPSSI energy range is likely due to the relatively low number of electrons detected by PEPSSI (10-100 per

integration period); the correlation increases when the PEPSSI data are binned in time to increase their signal-to-noise.

5.2. Upstream Magnetopause Crossing

At 17:50 UTC on DOY 056, at a distance of 67 R_J from Jupiter, the Alice background subtracted count rate increased from 7 cps to 7000 cps in 80 minutes. This sudden increase in count rate, shown in Fig. 5, is due to the increase in the energetic electron flux as *New Horizons* crossed the Jovian magnetopause. After this sharp initial increase, the count rate decreased for the next two hours, reaching a level of 2800 cps, before increasing again to a dead time corrected count rate of 15800 cps at which point the instrument was repeatedly tripped into safe mode producing a gap in the count rate data. The three electron detectors on PEPSSI all show similar behavior. The ratios of the Alice count rate and PEPSSI electron fluxes before and after the magnetopause crossings show a harder electron energy spectrum inside Jupiter’s magnetosphere. Again, there is a strong correlation between the Alice count rate and the PEPSSI E0 electron flux, with Pearson linear correlation coefficients of 0.89 for the 25-190 keV energy range, 0.89 for the 190-700 keV energy range, and 0.94 for the 700-1000 keV energy range.

The location of the Jovian magnetopause boundary is determined by the balance between the dynamic pressure of the solar wind and the internal pressure of the magnetosphere, which consists of dynamic, thermal, and magnetic components [Huddleston *et al.*, 1998]. Joy *et al.* [2002] performed a statistical analysis on all magnetopause crossings observed by the *Pioneer 10*, *Pioneer 11*, *Voyager 1*, *Voyager 2*, *Ulysses*, and *Galileo* spacecraft and found that the Jovian magnetopause boundary exhibits a bimodal distribution with the most probable standoff distances occurring at $92 \pm 6 R_J$ when the magnetosphere

was in an expanded state and $63 \pm 4 R_J$ when the magnetosphere was in a compressed state. The observed magnetopause location at $67 R_J$ implies that the magnetosphere was in a compressed configuration, as might be expected given the observation of the prior solar wind event.

The PEPSSI E0 electron fluxes also show dramatic spikes prior to the magnetopause crossing around DOY 056.25 and 056.35. *McNutt et al.* [2007] attributed this to either the Jovian bow shock crossing or to upstream events like those reported by *Haggerty and Armstrong* [1999]. Without data from a magnetometer, it is difficult to distinguish between these two possible scenarios. The distance of *New Horizons* from Jupiter during these two spikes, $75\text{--}79 R_J$, is consistent with the most probable bow shock distance for a compressed magnetosphere: $73 \pm 10 R_J$ [*Joy et al.*, 2002]. However, the onset of the spike at DOY 056.25 corresponds exactly to when the spacecraft was executing an 81° slew. There are no significant pointing changes that can explain the return back to the pre-spike flux or the subsequent spike at DOY 056.35. Furthermore, while the PEPSSI E0 detector high energy electron flux shows nearly a factor of 30 increase in flux, the E1 detector shows only a 50% increase and the E2 detector actually shows a 20% decrease. After the spacecraft slew, the boresights of the PEPSSI E0, E1, and E2 detectors were oriented 64° , 111° , and 148° from the *New Horizons*-Jupiter vector, respectively. This suggests that the flux increases PEPSSI observed are due to bursts of electrons streaming away from Jupiter. The lack of any detectable increase in the Alice count rate implies that these bursts are limited to electrons with energies below 1 MeV.

5.3. Dayside Magnetosphere

As *New Horizons* flew through the dayside magnetosphere, the energetic electron flux observed by Alice was quite intense. Alice repeatedly exceeded the count rate safety limit of 15000 counts s⁻¹, producing the large data gaps on DOY 057, 058, and 059 seen in Fig. 3. When the flux of energetic electrons was low enough to permit Alice to operate normally, the observed count rate was highly variable on timescales of minutes to hours, and there are numerous occurrences when the Alice count rate changes by a factor of 2 on timescales of 50-100 s. Figure 6 shows the Alice count rate during a typical 30-minute period on DOY 057 beginning at 20:25:00 UT.

5.4. Dusk Sector Current Sheet Crossings

After *New Horizons*' closest approach to Jupiter, the flux of energetic electrons was less intense. Figure 7 shows the Alice and PEPSSI E0 count rates from DOY 059.5–063, when *New Horizons* was in the dusk-to-midnight sector. For comparison, the count rates have been normalized to the average value between DOY 061.0–061.4. Clear peaks in the count rate were observed when *New Horizons* was near System III (1965) longitudes of $\lambda_{III}=130^\circ$ and $\lambda_{III}=280^\circ$. These peaks in count rate result from the center of the Jovian current sheet sweeping over the spacecraft twice per Jovian rotation. The count rate peak near $\lambda_{III}=130^\circ$ occurs when *New Horizons* crosses the center of the current sheet from the south to the north (in reality, New Horizons moves a relatively small distance north during one Jovian rotation period, while the current sheet sweeps rapidly over the spacecraft in an oscillatory manner). Likewise, the peak near $\lambda_{III}=280^\circ$ occurs when *New Horizons* crosses the center of the current sheet from the north moving to the south, i.e., the current sheet is moving northward over the spacecraft. Similar behavior has been

seen by the *Pioneer 10*, *Voyager 1*, *Voyager 2*, and *Galileo* spacecraft when they were near Jupiter’s rotational equator [Goertz *et al.*, 1976; Vogt *et al.*, 1979a, b; Vasyliūnas *et al.*, 1997; Waldrop *et al.*, 2005]. In total, Alice observed 10 current sheet crossings. PEPSSI also observed 10 current sheet crossings, five of which occurred during periods when Alice was not operating. The times of the observed current sheet crossings and the location of the *New Horizons* spacecraft in System III (1965) and JSO coordinates are given in Table 1.

5.4.1. Location of Current Sheet Crossings

The simplest model for Jupiter’s current sheet is that of a rigid sheet lying in the equator plane of the magnetic dipole field. The height of such a current sheet is given by:

$$Z_{rigid} = \rho \tan \theta \cos (\lambda - \lambda') \quad (2)$$

where ρ is the cylindrical radial distance, θ is the tilt of the magnetic dipole field, λ is the System III longitude, and λ' is the System III longitude at which the current sheet has its most northern (+Z) extent. For the VIP4 model of Jupiter’s magnetic field, $\theta = 9.52^\circ$ and $\lambda'_{VIP4} = 20.4^\circ$ [Connerney *et al.*, 1998]. Panel A in Figure 8 shows the difference in height between *New Horizons* and a rigid current sheet as a function of the spacecraft’s (cylindrical) radial distance at the time of the 15 current sheet crossings given in Table 1. Filled (open) symbols represent a crossing during which *New Horizons* went from being north (south) of the current sheet to south (north) of it. The total RMS error of the data points is 3.5 R_J and the difference increases roughly linearly with radial distance from Jupiter indicating that the actual current sheet does not lie in the dipole equator plane, but rather is warped or hinged northward.

A hinged current sheet lies in the magnetic dipole equator plane close to the planet, but at larger distances is warped into a plane that is parallel to either the rotational equator [Behannon *et al.*, 1981; Khurana, 1992] or the solar wind flow [Khurana and Schwarzl, 2005]. To date, the most accurate published model of the Jovian current sheet is that of Khurana and Schwarzl [2005], hereafter KS05. Their model is based on fits to 6328 current sheet crossings observed in magnetometer data from *Pioneer 10*, *Pioneer 11*, *Voyager 1*, *Voyager 2*, *Ulysses*, and *Galileo*. The height of the hinged current sheet in the KS05 model is given by their Eq. 13:

$$\begin{aligned}
 Z_{model} = & \left(\sqrt{\left(x_H \tanh \frac{x}{x_H} \right)^2 + y^2} \right) \tan \theta \cos (\lambda - \lambda') \\
 & + x \left(1 - \tanh \left| \frac{x_H}{x} \right| \right) \tan \theta_{Sun}
 \end{aligned} \tag{3}$$

where x and y are the JSO coordinates of the spacecraft, $x_H = 47 R_J$ is the characteristic hinging distance, and θ_{Sun} is the angle between the Jupiter-Sun vector and the rotational equator. During the *New Horizons* flyby, $\theta_{Sun} = -2.9^\circ$. KS05 also include the effects of the non-dipolar magnetic field line geometry and the time to propagate a signal from Jupiter to the current sheet along a magnetic field line. As such, λ' in Eq. 2 is no longer a constant and is instead given by

$$\lambda' = \lambda'_{VIP4} + \delta_{wave} + \delta_B + b_0 \tag{4}$$

where δ_{wave} is the shift of the prime meridian longitude due to the finite time to propagate a magnetic signal from Jupiter, δ_B is the shift due to the swept-back geometry of Jupiter's magnetic field lines, and b_0 is a constant offset term. Both δ_B and δ_{wave} are complicated

non-linear functions of local time and radial distance. We note that for δ_B , the value of the model parameter a_4 given in Table 1 of KS05 contains a typographical error. The correct value should be $a_4 = 0.0016$ (K. Khurana, personal communication, 2010).

Panel B of Fig. 8 shows the height difference between the observed current sheet location and the KS05 model. While the overall RMS error of $2.3 R_J$ is better than the simple rigid current sheet model (and even somewhat better than the value of the RMS error of fit for all data used by KS05), it is clear that the fit for N→S crossings (RMS of $3.3 R_J$) is systematically worse than that for S→N crossings (RMS of $0.8 R_J$). This implies that one or more of the terms in Eq. 4 require modification to better match the effective prime meridian of the current sheet during the *New Horizons* flyby. Since the data used to derive the parameters of the KS05 model were obtained over a large range of local times, radial distances, and solar wind conditions, this is not particularly surprising.

The full KS05 model is governed by 24 parameters. With only 15 current sheet crossings observed along a single trajectory, the KS05 model is significantly under-determined by the *New Horizons* current sheet data. We therefore take the simplest approach of allowing the constant offset term in Eq 4, b_0 , to vary to match the data. We find a value of $b_0 = 12.0^\circ$ yields the best fit and results in a N→S RMS of $2.4 R_J$, a S→N RMS of $2.0 R_J$, and a combined RMS of $2.2 R_J$, as shown in Fig. 8, panel C. Like the rigid current sheet case shown in panel A, all of the observed current sheet crossings, even those at $35 R_J$, have been displaced northwards of the predicted locations. Given that the Z-component of the solar wind velocity is also in the northward direction, the most plausible explanation is that the current sheet has been pushed northwards by the solar wind.

It has long been recognized that the hinging distance of the current sheet, x_H will vary in response to the solar wind dynamic pressure, moving outward when the solar wind pressure is low and inward when the solar wind pressure is high [Goertz, 1981]. Given that the mSWiM model predicts a factor of ~ 80 increase in the solar wind dynamic pressure at Jupiter, with elevated levels remaining until DOY 062, it is quite plausible that the hinging distance during the *New Horizons* flyby would be smaller than the value of $x_H = 47 R_J$ found by KS05. We therefore allow both b_0 and x_h to vary and find best-fit values of $b_0 = 12.5^\circ$ and $x_H = 5.0 R_J$. This combination of model parameters yields a combined RMS value of $0.6 R_J$ N \rightarrow S, $0.5 R_J$ S \rightarrow N, and $0.6 R_J$ total—a noticeably better fit, with no clear systematic deviations—as shown in panel D. (Note, we strongly caution against extrapolating these fit results radially inwards of the observed *New Horizons* current sheet crossings. There, strong centrifugal forces will confine the current sheet to the “centrifugal equator”, the locus of points that are most distant from Jupiter’s spin axis along a given magnetic field line.) Thus, it seems highly likely that the solar wind influences the location of the current sheet even to radial distances as small as $\sim 35 R_J$.

5.4.2. Thickness of the Dusk Current Sheet

Initially, the count rate peaks associated with current sheet crossings are relatively broad (cf. Fig. 7). At the minima between peaks, both Alice and PEPSSI count rates remain significantly elevated above their pre-magnetopause crossing levels, with count rates only a few times lower than their peak values. This suggests that initially, at least, *New Horizons* did not exit the current sheet and enter into the lobe regions, although from the low count rates on DOY 060.9 and DOY 061.3, it appears that the spacecraft came close to entering the southern lobe region. This implies that the current sheet in

this sector of the dusk magnetosphere is thicker than its vertical motion over the course of one Jovian rotation.

Although we cannot directly measure the current sheet thickness with Alice or PEPSSI data, we can estimate the height of the center of the current sheet using the modified KS05 current sheet model described in Section 5.4.1 above. Using the best-fit model parameters of $x_H = 5.0 R_J$ and $b_0 = 12.5^\circ$, the center of the current sheet was $7.4 R_J$ north the spacecraft on DOY 060.9 (when *New Horizons* appears to be closest to leaving the current sheet), and thus the half-thickness of the current sheet at this location must be at least as great. This is consistent with data from the *Ulysses* Energetic Particle Composition Instrument and the *Galileo* magnetometer that also suggest a thick current sheet in the dusk sector [Krupp *et al.*, 1999; Kivelson and Khurana, 2002].

However, a rapid transition in the current sheet appears to have occurred around DOY 062, when the spacecraft was at a local time of ~ 2200 LT and a radial distance of $\sim 70 R_J$. The count rate peak corresponding to the current sheet crossing on DOY 061.86 is broad, similar to previous count rate peaks, and indicative of a thick current sheet. However, the next four current sheet crossings all have count rate peaks that are much narrower, and between peaks, the count rates fall to the lowest levels seen inside the Jovian magnetosphere (an Alice count rate of ~ 150 cps). This low flux of energetic electrons is consistent with *New Horizons* having entered the lobe regions, where magnetic field lines are open and energetic particles are quickly lost. Using the modified KS05 model, we estimate the current sheet half thickness in this region to be $\sim 3.4 R_J$ —a value intermediate between the $>7.4 R_J$ observed earlier and the half thickness of $<1.5 R_J$ typical of the dawn sector.

There is some evidence for a similarly abrupt current sheet transition in *Galileo* magnetometer data. Beyond a radial distance of $30 R_J$, the magnetic pressure at the center of the was observed to decrease suddenly around 2100 LT [Kivelson and Khurana, 2002]. One interpretation of this result is that plasma has gone from being more distributed along the flux tube to being more concentrated in the equatorial region, i.e., the current sheet has gone from being thicker and relatively diffuse to thinner and more dense. However, if the plasma densities were actually higher at the center of the current sheet, one would expect the Alice and PEPSSI count rates to be significantly higher than observed previously when the plasma was more diffuse. Instead, the peak energetic electron fluxes are comparable to previous maxima, suggesting that the plasma density at the center of the current sheet hasn't changed significantly, though the sheet is thinner, which in turn implies a lowered flux tube content. Intriguingly, the sudden thinning of the current sheet corresponds to the arrival of a solar wind reverse shock (lower dynamic pressure following the shock) predicted by the mSWiM model to arrive at Jupiter on DOY 061.9.

6. Conclusions

The Alice FUV spectrograph on *New Horizons* provides a novel means of detecting 1-8 MeV electrons at Jupiter. Taken as a whole, the Alice count rate data, in combination with the PEPSSI electron data, show the response of the Jovian magnetosphere to a period of disturbed solar wind flow. Fortuitous timing and the high flyby velocity of the spacecraft enabled *New Horizons* to directly observe a solar wind compression event pass over the spacecraft and subsequently fly through the Jovian magnetopause, the outer-to-middle magnetosphere, and the dusk sector current sheet while the solar wind dynamic pressure remained at elevated levels. The location of the upstream magnetopause crossing at $67 R_J$

(and possibly the bow shock crossing at 75-79 R_J) is consistent with the magnetosphere being in a compressed configuration. The northerly displacement of the 15 observed current sheet crossings suggests the influence of the solar wind, even at radial distances as small as 35 R_J . An abrupt thinning of the current sheet was observed around 2200 LT (72 R_J), when the half-thickness of the current sheet decreased from $>7.4 R_J$ to $\sim 3.4 R_J$ over a few hours in elapsed time, a few R_J in radial distance, and a few minutes in local solar time. We propose that this thinning is due to a temporal change, possibly associated with the predicted arrival of a solar wind reverse shock.

Acknowledgments. We would like to thank the *New Horizons* science and mission teams and acknowledge the financial support of the *New Horizons* mission by NASA. AJS and ABS gratefully acknowledge support from the NASA Jupiter Data Analysis Program (NNX09AE05G). We kindly thank Fran Bagenal, Peter Delamere, Mariel Desroche, Caitriona Jackman, and Krishan Khurana for many helpful discussions and K.C. Hansen and B. Zieger for providing solar wind propagations from their Michigan Solar Wind Model (<http://mswim.engin.umich.edu/>).

References

- Baker, D. N., and J. A. van Allen (1976), Energetic electrons in the Jovian magnetosphere, *J. Geophys. Res.*, , 81, 617–632, doi:10.1029/JA081i004p00617.
- Baker, D. N., R. D. Zwickl, S. M. Krimigis, J. F. Carbary, and M. H. Acuna (1984), Energetic particle transport in the upstream region of Jupiter - Voyager results, *J. Geophys. Res.*, , 89, 3775–3787, doi:10.1029/JA089iA06p03775.
- Behannon, K. W., L. F. Burlaga, and N. F. Ness (1981), The Jovian magnetotail and its

current sheet, *J. Geophys. Res.*, , 86, 8385–8401, doi:10.1029/JA086iA10p08385.

Berger, M., J. Coursey, M. Zucker, and J. Chang (2005), ESTAR, PSTAR, and ASTAR:

Computer programs for calculating stopping-power and range tables for electrons, pro-

tons, and helium ions, [Online] Available: <http://physics.nist.gov/Star> [2010, April 06].

Clarke, J. T., J. Nichols, J.-C. Gérard, D. Grodent, K. C. Hansen, W. Kurth, G. R. Glad-

stone, J. Duval, S. Wannawichian, E. Bunce, S. W. H. Cowley, F. Crary, M. Dougherty,

L. Lamy, D. Mitchell, W. Pryor, K. Retherford, T. Stallard, B. Zieger, P. Zarka,

and B. Cecconi (2009), Response of Jupiter’s and Saturn’s auroral activity to the

solar wind, *Journal of Geophysical Research (Space Physics)*, 114, A05,210, doi:

10.1029/2008JA013694.

Connerney, J. E. P., M. H. Acuña, N. F. Ness, and T. Satoh (1998), New models of

Jupiter’s magnetic field constrained by the Io flux tube footprint, *J. Geophys. Res.*,

103, 11,929–11,940.

Elliott, H. A., D. J. McComas, P. W. Valek, F. Allegrini, F. J. Crary, F. Bagenal, R. Glad-

stone, S. A. Livi, and J. T. Clarke (2007), Solar wind conditions near jupiter measured

with the solar wind around pluto (SWAP) instrument on New Horizons, in *Magneto-*

spheres of the Outer Planets 2007, San Antonio, TX.

Gladstone, G. R., S. A. Stern, D. C. Slater, M. Versteeg, M. W. Davis, K. D. Retherford,

L. A. Young, A. J. Steffl, H. Throop, J. W. Parker, H. A. Weaver, A. F. Cheng, G. S.

Orton, J. T. Clarke, and J. D. Nichols (2007), Jupiter’s Nightside Airglow and Aurora,

Science, 318, 229–, doi:10.1126/science.1147613.

Goertz, C. K. (1981), The orientation and motion of the predawn current

sheet and Jupiter’s magnetotail, *J. Geophys. Res.*, , 86, 8429–8434, doi:

10.1029/JA086iA10p08429.

Goertz, C. K., B. A. Randall, M. F. Thomsen, D. E. Jones, and E. J. Smith (1976),
Evidence for open field lines in Jupiter’s magnetosphere, *J. Geophys. Res.*, , 81, 3393–
3397, doi:10.1029/JA081i019p03393.

Greathouse, T. K., G. R. Gladstone, J. I. Moses, S. A. Stern, K. D. Retherford, R. J. Ver-
vack, D. C. Slater, M. H. Versteeg, M. W. Davis, L. A. Young, A. J. Steffl, H. Throop,
and J. W. Parker (2010), New Horizons Alice ultraviolet observations of a stellar occul-
tation by Jupiter’s atmosphere, *Icarus*, 208, 293–305, doi:10.1016/j.icarus.2010.02.002.

Haggerty, D., and T. P. Armstrong (1999), Observations of Jovian upstream events by
Ulysses, *J. Geophys. Res.*, 104, 4629–4642, doi:10.1029/1998JA900148.

Heynderickx, D., B. Quaghebeur, E. Speelman, H. D. R. Evans, and E. J. Daly (2001),
Spacecraft Charging Models in ESA’s Space Environment Information System (SPEN-
VIS), in *Spacecraft Charging Technology, ESA Special Publication*, vol. 476, edited by
R. A. Harris, p. 163.

Huddleston, D. E., C. T. Russell, M. G. Kivelson, K. K. Khurana, and L. Bennett (1998),
Location and shape of the Jovian magnetopause and bow shock, *J. Geophys. Res.*, ,
103, 20,075–20,082, doi:10.1029/98JE00394.

Joy, S. P., M. G. Kivelson, R. J. Walker, K. K. Khurana, C. T. Russell, and T. Ogino
(2002), Probabilistic models of the Jovian magnetopause and bow shock locations, *Jour-
nal of Geophysical Research (Space Physics)*, 107, 1309, doi:10.1029/2001JA009146.

Khurana, K. K. (1992), A generalized hinged-magnetodisc model of Jupiter’s nightside
current sheet, *J. Geophys. Res.*, , 97, 6269–6276, doi:10.1029/92JA00169.

- 543 Khurana, K. K., and H. K. Schwarzl (2005), Global structure of Jupiter’s magnetospheric
544 current sheet, *Journal of Geophysical Research (Space Physics)*, *110*(A9), 7227, doi:
545 10.1029/2004JA010757.
- 546 Kivelson, M. G., and K. K. Khurana (2002), Properties of the magnetic field in the
547 Jovian magnetotail, *Journal of Geophysical Research (Space Physics)*, *107*, 1196, doi:
548 10.1029/2001JA000249.
- 549 Knoll, G. F. (1979), *Radiation detection and measurement*.
- 550 Krupp, N., M. K. Dougherty, J. Woch, R. Seidel, and E. Keppler (1999), Energetic
551 particles in the duskside Jovian magnetosphere, *J. Geophys. Res.*, , *104*, 14,767–14,780,
552 doi:10.1029/1999JA900156.
- 553 Lei, F., P. R. Truscott, C. S. Dyer, B. Quaghebeur, D. Heynderickx, P. Niemi-
554 nen, H. Evans, and E. Daly (2002), MULASSIS: a geant4-based multilayered shield-
555 ing simulation tool, *IEEE Transactions on Nuclear Science*, *49*, 2788–2793, doi:
556 10.1109/TNS.2002.805351.
- 557 Lucke, R. L. (1976), Counting statistics for nonnegligible dead time corrections, *Review*
558 *of Scientific Instruments*, *47*, 766–767, doi:10.1063/1.1134733.
- 559 McComas, D., F. Allegrini, F. Bagenal, P. Casey, P. Delamere, D. Demkee, G. Dunn,
560 H. Elliott, J. Hanley, K. Johnson, J. Langle, G. Miller, S. Pope, M. Reno, B. Rodriguez,
561 N. Schwadron, P. Valek, and S. Weidner (2008), The Solar Wind Around Pluto (SWAP)
562 Instrument Aboard New Horizons, *Space Sci. Rev.*, *140*, 261–313, doi:10.1007/s11214-
563 007-9205-3.
- 564 McComas, D. J., F. Allegrini, F. Bagenal, F. Crary, R. W. Ebert, H. Elliott, A. Stern, and
565 P. Valek (2007), Diverse Plasma Populations and Structures in Jupiter’s Magnetotail,

Science, *318*, 217–, doi:10.1126/science.1147393.

McNutt, R. L., D. K. Haggerty, M. E. Hill, S. M. Krimigis, S. Livi, G. C. Ho, R. S. Gurnee, B. H. Mauk, D. G. Mitchell, E. C. Roelof, D. J. McComas, F. Bagenal, H. A. Elliott, L. E. Brown, M. Kusterer, J. Vande-griff, S. A. Stern, H. A. Weaver, J. R. Spencer, and J. M. Moore (2007), Energetic Particles in the Jovian Magnetotail, *Science*, *318*, 220–, doi:10.1126/science.1148025.

McNutt, R. L., S. A. Livi, R. S. Gurnee, M. E. Hill, K. A. Cooper, G. B. Andrews, E. P. Keath, S. M. Krimigis, D. G. Mitchell, B. Tossman, F. Bagenal, J. D. Boldt, W. Bradley, W. S. Devereux, G. C. Ho, S. E. Jaskulek, T. W. Lefevre, H. Malcom, G. A. Marcus, J. R. Hayes, G. T. Moore, M. E. Perry, B. D. Williams, P. Wilson, L. E. Brown, M. B. Kusterer, and J. D. Vande-griff (2008), The Pluto Energetic Particle Spectrometer Science Investigation (PEPSSI) on the New Horizons Mission, *Space Sci. Rev.*, *140*, 315–385, doi:10.1007/s11214-008-9436-y.

Retherford, K. D., J. R. Spencer, S. A. Stern, J. Saur, D. F. Strobel, A. J. Steffl, G. R. Gladstone, H. A. Weaver, A. F. Cheng, J. W. Parker, D. C. Slater, M. H. Versteeg, M. W. Davis, F. Bagenal, H. B. Throop, R. M. C. Lopes, D. C. Reuter, A. Lunsford, S. J. Conard, L. A. Young, and J. M. Moore (2007), Io’s Atmospheric Response to Eclipse: UV Aurorae Observations, *Science*, *318*, 237–, doi:10.1126/science.1147594.

Riddle, A. C., and J. W. Warwick (1976), Redefinition of System III longitude, *Icarus*, *27*, 457–459, doi:10.1016/0019-1035(76)90025-7.

Schardt, A. W., F. B. McDonald, and J. H. Trainor (1981), Energetic particles in the predawn magnetotail of Jupiter, *J. Geophys. Res.*, *86*, 8413–8428, doi:10.1029/JA086iA10p08413.

- 589 Stern, S. A. (2008), The New Horizons Pluto Kuiper Belt Mission: An Overview with
590 Historical Context, *Space Sci. Rev.*, *140*, 3–21, doi:10.1007/s11214-007-9295-y.
- 591 Stern, S. A., D. C. Slater, J. Scherrer, J. Stone, G. Dirks, M. Versteeg, M. Davis, G. R.
592 Gladstone, J. W. Parker, L. A. Young, and O. H. W. Siegmund (2008), ALICE: The
593 Ultraviolet Imaging Spectrograph Aboard the New Horizons Pluto-Kuiper Belt Mission,
594 *Space Sci. Rev.*, *140*, 155–187, doi:10.1007/s11214-008-9407-3.
- 595 Vasyliūnas, V. M., L. A. Frank, K. L. Ackerson, and W. R. Paterson (1997), Geome-
596 try of the plasma sheet in the midnight-to-dawn sector of the Jovian magnetosphere:
597 Plasma observations with the Galileo spacecraft, *Geophys. Res. Lett.*, , *24*, 869–872,
598 doi:10.1029/97GL00757.
- 599 Vogt, R. E., W. R. Cook, A. C. Cummings, T. L. Garrard, N. Gehrels, E. C. Stone, J. H.
600 Trainor, A. W. Schardt, T. Conlon, N. Lal, and F. B. McDonald (1979a), Voyager 1
601 - Energetic ions and electrons in the Jovian magnetosphere, *Science*, *204*, 1003–1007,
602 doi:10.1126/science.204.4396.1003.
- 603 Vogt, R. E., A. C. Cummings, T. L. Garrard, N. Gehrels, E. C. Stone, J. H. Trainor,
604 A. W. Schardt, T. F. Conlon, and F. B. McDonald (1979b), Voyager 2 - Ener-
605 getic ions and electrons in the Jovian magnetosphere, *Science*, *206*, 984–987, doi:
606 10.1126/science.206.4421.984.
- 607 Waldrop, L. S., T. A. Fritz, M. G. Kivelson, K. Khurana, N. Krupp, and A. Lagg (2005),
608 Jovian plasma sheet morphology: particle and field observations by the Galileo space-
609 craft, *Planet. Space Sci.*, *53*, 681–692, doi:10.1016/j.pss.2004.11.003.
- 610 Zieger, B., and K. C. Hansen (2008), Statistical validation of a solar wind propagation
611 model from 1 to 10 AU, *Journal of Geophysical Research (Space Physics)*, *113*, 8107,

⁶¹² doi:10.1029/2008JA013046.

Table 1. Times and locations of *New Horizons* during current sheet crossings

DOY	ρ_{III} (R _J)	λ_{III} (°)	Z_{III} (R _J)	x_{JSO} (R _J)	y_{JSO} (R _J)	z_{JSO} (R _J)
59.753 [†]	34.4	142.7	-2.8	-9.1	33.1	-3.9
59.900 [†]	35.8	265.1	-2.5	-12.8	33.4	-3.8
60.179	39.3	138.4	-1.9	-19.8	33.8	-3.6
60.336	41.6	271.2	-1.6	-23.7	34.0	-3.4
60.590 [†]	45.6	125.5	-1.1	-30.0	34.2	-3.2
60.771	48.8	279.2	-0.7	-34.4	34.4	-3.1
61.027	53.5	137.9	-0.1	-40.7	34.6	-2.9
61.190	56.6	276.8	0.2	-44.6	34.7	-2.7
61.431	61.3	123.7	0.7	-50.5	34.8	-2.5
61.603	64.8	271.2	1.1	-54.6	34.9	-2.3
61.861 [†]	70.1	133.3	1.7	-60.8	34.9	-2.1
62.033	73.7	281.5	2.0	-64.8	35.0	-1.9
62.269	78.7	125.1	2.5	-70.4	35.1	-1.7
62.453	82.6	284.1	2.9	-74.8	35.1	-1.6
62.686 [†]	87.6	125.3	3.4	-80.3	35.2	-1.3

[†] Current sheet crossing derived from PEPSSI electron data

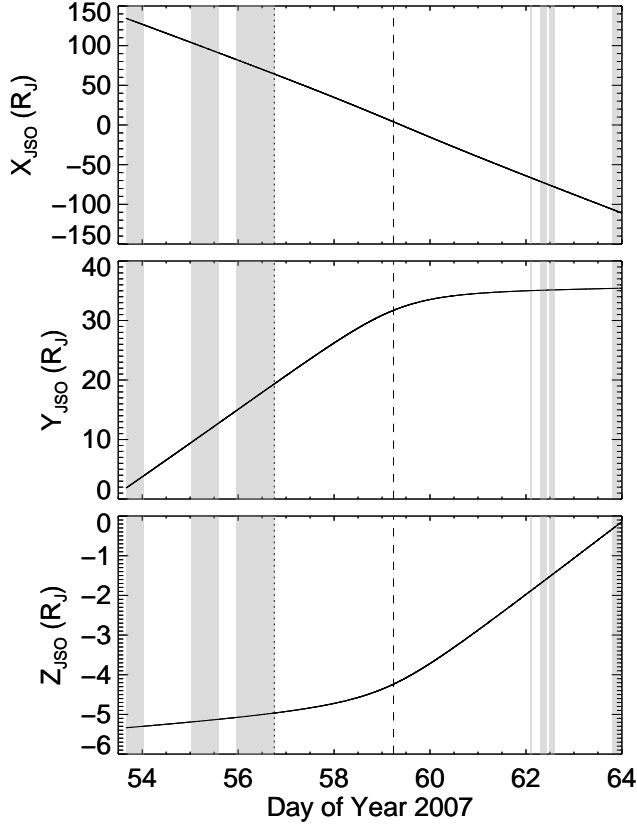


Figure 1. Trajectory of the *New Horizons* spacecraft during the Alice observing period. Distances are jovicentric and given in the Jupiter-Solar-Orbital coordinate system (+X to the Sun, +Z perpendicular to the orbit plane of Jupiter near the north rotational pole, and +Y completing the triad in the direction roughly opposite of Jupiter’s orbital motion). The magnetopause crossing is marked by a dotted vertical line and the closest approach to Jupiter is marked with a dashed line. Shaded areas indicate periods when Alice was taking data and the energetic electron flux is consistent with *New Horizons* being on open magnetic field lines. $1 R_J = 71,492$ km

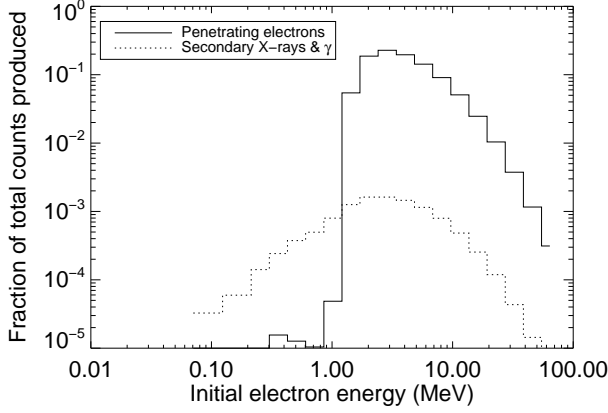


Figure 2. Fraction of the total number of Alice counts produced by penetrating electrons and secondary X-rays and γ -rays as a function of initial electron energy. The electrons are assumed to have an energy spectrum like that observed in the Jovian magnetosphere by *Pioneer 10* [Baker and van Allen, 1976]. This analysis does not include the effect of fluorescence from the window in the detector door. The efficiency of the Alice detector is taken to be 0.33 for electrons and 0.02 for X-rays and γ -rays (see text in Section 2 for details). 90% of detected counts are produced by electrons with initial energies between 1-8 MeV. Electrons with initial energies as low as 50 keV can produce secondary photons that can be detected, but their effect on the total count rate is negligible.

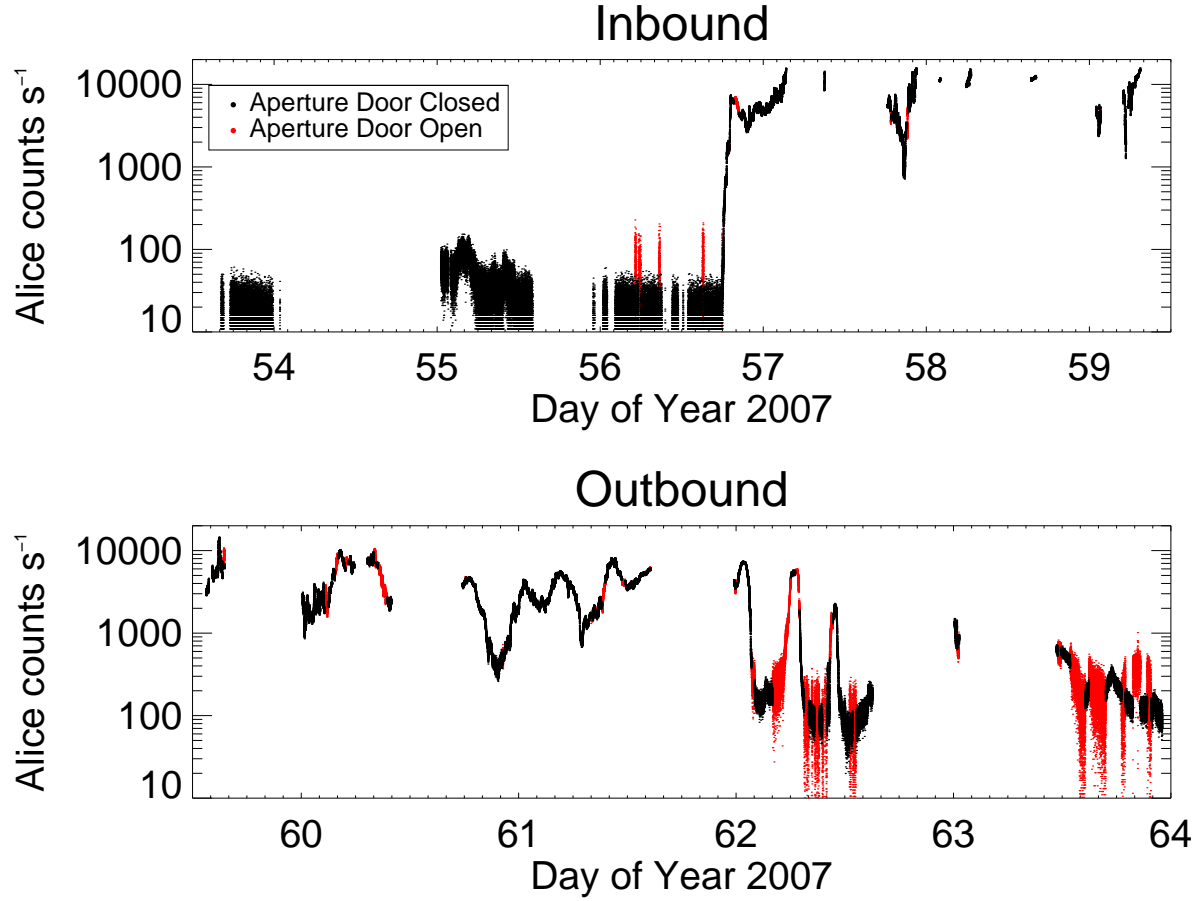


Figure 3. The count rate of Alice recorded in housekeeping data during the Jupiter flyby. The data have been corrected for detector dead time and have had the background count rate and stim pulse rate subtracted. Data obtained when the Alice aperture door was closed are colored black; data obtained when the aperture door was open are colored red. The count rate produced by FUV photons during the door open periods was estimated by comparing the count rate immediately before/after the aperture door opened/closed and subtracted from the data.

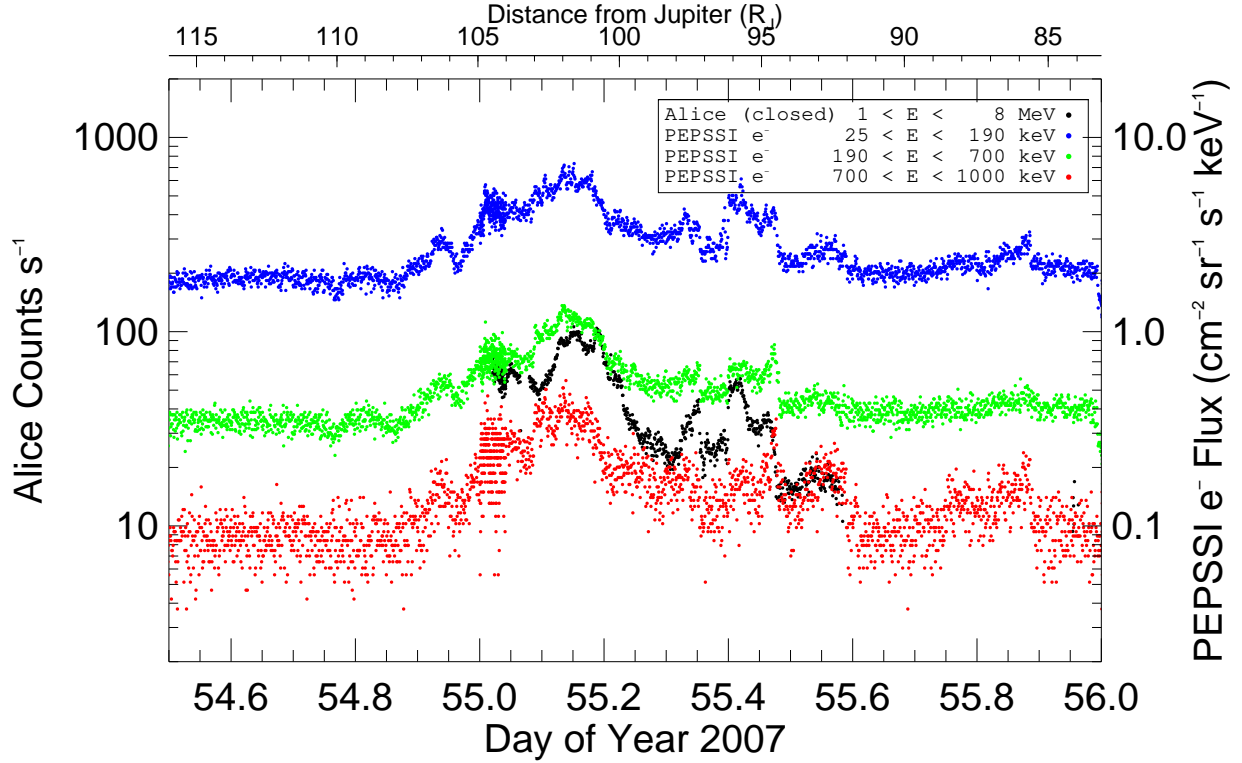


Figure 4. Dead time corrected, background subtracted Alice count rates and PEPSSI electron fluxes, on day 55. PEPSSI electron data have been averaged over the three electron detectors. During this period, New Horizons was upstream of the Jovian magnetosphere and immersed in the solar wind plasma. Alice count rates have been averaged to match the 60-second sampling of the PEPSSI data during this period. Electron fluxes for PEPSSI’s three energy ranges are shown in red, green, and blue.

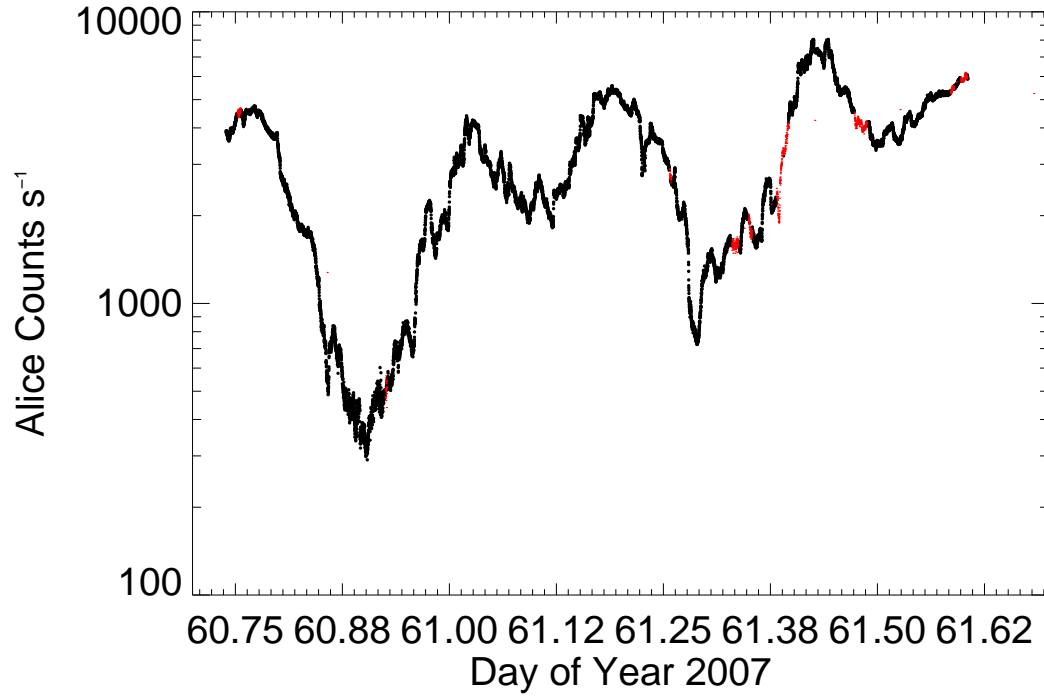


Figure 5. Dead time corrected, background subtracted Alice count rates and PEPSSI electron fluxes around the time of the Jovian magnetopause crossing. The good match between Alice data obtained with the aperture door opened (black) and closed (orange) demonstrates the validity of the technique used to subtract the FUV photon count rate described in Section 3.3. Alice count rates have been averaged to match the 60-second sampling of the PEPSSI data during this period. Electron fluxes for PEPSSI’s three energy ranges are shown in red, green, and blue.

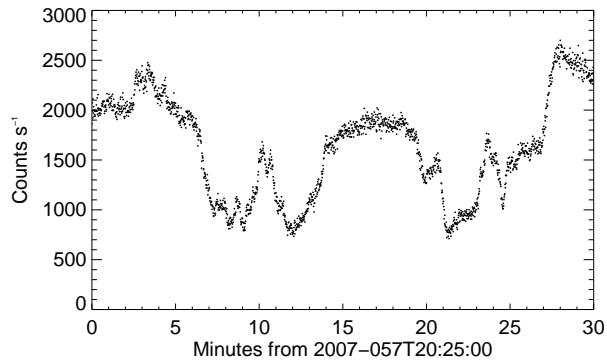


Figure 6. Dead time corrected, background subtracted Alice count rate during a 30-minute period showing factor of two changes in count rate on timescales of a few minutes. During these observations, *New Horizons* was located $46.3 R_J$ from Jupiter at approximately 1400 LT.

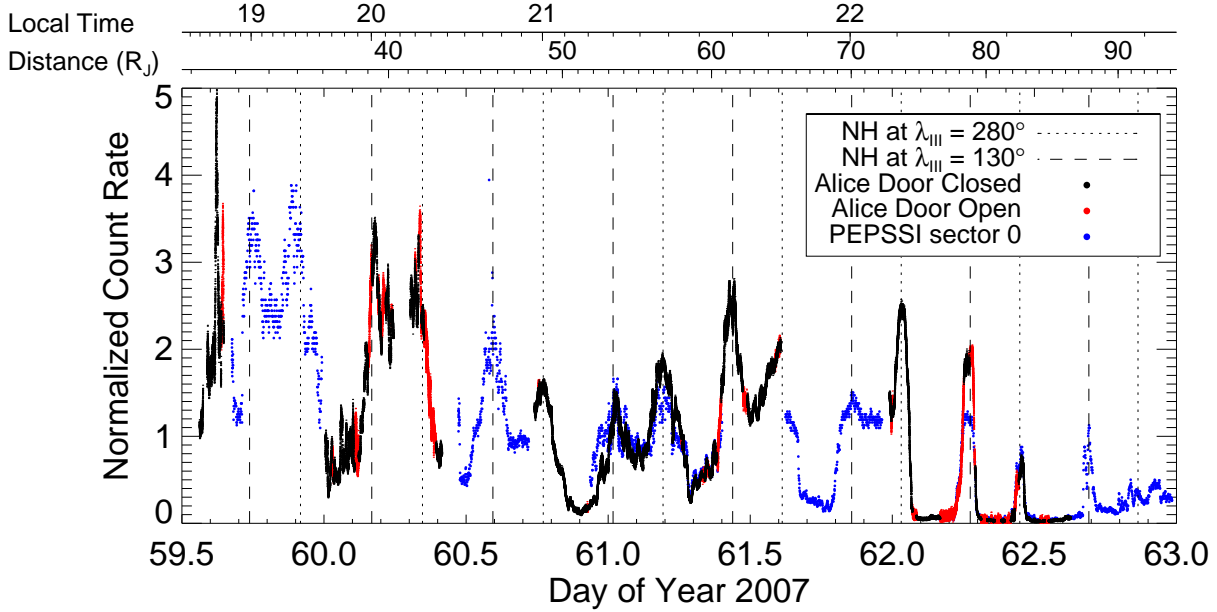


Figure 7. Count rates for Alice and the PEPSSI E0 700-1000 keV energy range. Count rates have been normalized to the average between DOY 61.0 and 61.4. The absolute count rate of Alice is approximately 170 times greater than the absolute count rate in the PEPSSI E0 700-1000 keV energy range. The two axes above the plot show the local time of *New Horizons*, and the (spherical) radial distance from Jupiter in R_J . Times when the *New Horizons* spacecraft was located at $\lambda_{III} = 130^\circ$ and $\lambda_{III} = 280^\circ$ are marked by dashed and dotted lines, respectively. Black dots represent count rates obtained when the Alice aperture door was closed and no FUV photons could reach the detector. Red dots represent the Alice count rate when the aperture door was open, after correcting for counts due to FUV photons. The energetic electron flux at *New Horizons* shows a clear, double-peaked 10-hr periodicity corresponding to the Jovian current sheet sweeping over the spacecraft twice per Jovian rotation.

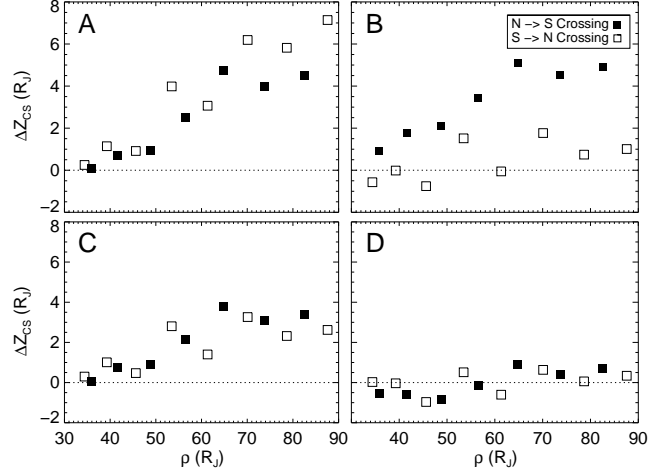


Figure 8. Residuals between the height of *New Horizons* above the rotational equator during the current sheet crossings listed in Table 1 and the height of model current sheets. Filled symbols represent N→S crossings, and open symbols represent S→N crossings. Panel A shows the residuals for a current sheet located in the magnetic dipole equator plane. Panel B shows residuals for the current sheet model of *Khurana and Schwarzl* [2005]. Panel C shows residuals using the KS05 model and a value of $b_0 = 12.0^\circ$, which minimizes the difference between N→S and S→N crossings. Panel D shows the difference using the KS05 model with $b_0 = 12.5^\circ$ and a characteristic hinging distance, $x_H = 5 R_J$.